Physical ageing and creep in PVC

B. E. Read, G. D. Dean, P. E. Tomlins* and J. L. Lesniarek-Hamid
Division of Materials Metrology, National Physical Laboratory, Teddington, Middlesex, TW11 0LW, UK
(Received 2 August 1991; accepted 1 October 1991)

Tensile creep compliances have been determined for PVC over a wide range of times ($t = 10^{-8}$ to 10^{6} s) at 23°C. Results were obtained on samples of different age characterized by the elapsed time t_e between quenching from 85°C and the instant of load application. Various empirical functions were employed to model the data from both short-term ($t \leqslant 0.2t_e$) and long-term ($t > 0.2t_e$) tests in terms of compliance contributions from secondary (β) and glass–rubber (α) retardation regions. Results of these analyses suggest that physical ageing produces a decrease in strength of the β-process, an increase in average retardation time for the α-process and negligible changes in the widths of the respective retardation time distributions. Comments are made on the structural significance of the results for the β-process and on the validity of functions used to describe the creep curves.

(Keywords: creep; PVC; physical ageing)

INTRODUCTION

In previous publications[1–5] we have considered the physical ageing and creep of glassy polymers after cooling from a temperature T_o to the temperature T ($T_\beta \leqslant T < T_g < T_o$) at which the ageing and subsequent creep experiments are performed. Here T_g is the glass transition temperature and T_β is the temperature at which the secondary (β) relaxation region is observed in low frequency dynamic tests. The age of a polymer sample at the start of a creep test is specified by the elapsed time t_e between cooling from T_o to T and the instant of load application.

Over wide ranges of creep time t the tensile creep compliance $D(t)$ can be expressed in the form:

$$D(t) = D_{U\beta} + D_\beta(t) + D_\alpha(t) \qquad (1)$$

where $D_{U\beta}$ is the unrelaxed compliance at short times and $D_\beta(t)$ and $D_\alpha(t)$ are respective compliance contributions from overlapping secondary (β) and glass–rubber (α) retardation processes. During short-term creep tests ($t \leqslant 0.2t_e$) changes in age state of the polymer are negligible and the following empirical expressions were found convenient in modelling the data for several polymers[2–5]:

$$D_\beta(t) = (D_{R\beta} - D_{U\beta})\frac{(t/\tau_\beta)^n[(t/\tau_\beta)^n + \cos(n\pi/2)]}{1 + 2(t/\tau_\beta)^n\cos(n\pi/2) + (t/\tau_\beta)^{2n}}$$
$$= \Delta D_\beta \psi_\beta(t) \qquad (2)$$

and

$$D_\alpha(t) = (D_{R\alpha} - D_{R\beta})[1 - \exp - (t/\tau_\alpha)^m]$$
$$= \Delta D_\alpha \psi_\alpha(t) \qquad (3)$$

In these equations $D_{R\beta}$ and $D_{R\alpha}$ are the relaxed compliances of the β- and α-processes, respectively, $\Delta D_\beta (= D_{R\beta} - D_{U\beta})$ and $\Delta D_\alpha (= D_{R\alpha} - D_{R\beta})$ are the retardation strengths and τ_β and τ_α are mean retardation times. The constants n ($0 < n \leqslant 1$) and m ($0 < m \leqslant 1$) are distribution parameters which decrease in magnitude as the widths of the respective β- and α-retardation spectra increase. Note that the creep functions $\psi_\beta(t)$ and $\psi_\alpha(t)$ are consistent with the well known Cole–Cole and Williams–Watts retardation functions respectively[5,6].

The influence of physical ageing on short-term creep may be considered in terms of possible variations with t_e in ΔD_β and ΔD_α (or limiting compliances $D_{U\beta}$, $D_{R\beta}$ and $D_{R\alpha}$), retardation times and distribution parameters. For secondary processes in glassy polymers, available evidence[5,7–9] suggests that τ_β and n are essentially independent of t_e. There are differing views, however, as to whether ΔD_β remains constant[7] or decreases significantly[5,8,9] with increasing t_e.

For the glass–rubber retardation, it is widely accepted that physical ageing produces an increase in retardation time τ_α and that ΔD_α and the shape of the distribution of retardation times and hence the parameter m are unaffected[10]. This conclusion is consistent with the success at superposing short-term $D_\alpha(t)$ *versus* $\log t$ curves, determined at different t_e, by horizontal shifts along the $\log t$ axis[1]. However these curves may also be superposed by relative vertical scalings, indicating that ΔD_α could decrease with increasing t_e. It has also been claimed[11] that physical ageing gives rise to some broadening of the α-retardation, corresponding to a decrease in m.

If ΔD_α is assumed to be unaffected by ageing, then the following relation is also convenient for modelling short-term creep in the glass–rubber region of amorphous polymers:

$$D(t) = [D_{U\beta} + D_\beta(t)]\exp(t/t_o)^\gamma \qquad (4)$$

Here the relaxation time t_o and distribution parameter γ

*To whom correspondence should be addressed

0032-3861/92/132689-10

$(0 < \gamma \leqslant 1)$ for the α-process may each depend on t_e. For negligible overlap between the β- and α-regions, equation (4) becomes:

$$D(t) = D_{R\beta} \exp(t/t_o)^{\gamma} \quad (5)$$

This equation has been widely employed by Struik[10] and is consistent with the stress relaxation function, $\exp -(t/t_o)^{\gamma}$, proposed by Kohlrausch[11,12].

The validity of empirical functions and age-dependence of retardation parameters for the α-process can be further explored through an analysis of long-term $(t > 0.2t_e)$ creep data. This requires modifications to equations (2), (3), (4) and (5) to allow for possible variations in parameters due to further ageing during the creep[6]. In this context, long-term creep in amorphous polymers has been predicted with reasonable accuracy from short-term data on the basis of equation (5) assuming[3,5] that ΔD_α and γ are constant and that t_o increases with t. For semicrystalline poly(butylene terephthalate)[4], long-term creep involving the glass–rubber process was predicted quite accurately using a modification to equation (3) assuming that τ_α increased with t at constant ΔD_α and m. However, no predictions have been published of the long-term creep of glassy polymers on the basis that ΔD_α may decrease with increasing age.

To obtain further insight into the quantitative effects of physical ageing, and the validity of empirical creep functions for glassy polymers, detailed analyses have recently been undertaken of short-term and long-term creep data for PVC. The data were obtained over a wide time range (10^{-8} to 10^6 s) at low stress levels ($\leqslant$5.1 MPa) using a combination of static and dynamic techniques. In this paper the data and the analyses are presented and discussed. The results have an important bearing on the prediction of long-term creep from short-term tests and on the non-linear creep behaviour at high stresses which is discussed in a separate publication[13].

EXPERIMENTAL

Material and procedures

The PVC (ICI Darvic) was obtained in the form of a 6 mm thick, transparent sheet from Amari Plastics. It had been stored in the laboratory for a period of about 10 years before commencing the present project. Strips of different dimensions were machined from the sheet for the various dynamic and creep measurements. The measured density of original specimens at 23°C was 1387 kg m^{-3}. A loss factor *versus* temperature plot, determined by a dynamic mechanical method at 1 Hz, exhibited maxima at $T_\alpha (\approx T_g) = 84$°C and $T_\beta = -50$°C.

Before making the creep and dynamic measurements, specimens were heated to the temperature $T_o = 85$°C for a period of 30 min to erase previous ageing effects. They were then quenched in water at room temperature and stored in air at 23°C for periods of elapsed time t_e ranging from 2.5–240 h before testing. One specimen was quenched in air at room temperature to assess, on the basis of audiofrequency measurements, whether internal stresses might be affecting data for the water-quenched specimens.

Measurement of creep compliance

For creep times $t \geqslant 1$ s, $D(t)$ values at 23°C were obtained from measurements[6] of the time-dependent extension of strips subjected to a constant stress of 5.1 MPa. This stress level produced quite low strains (0.15–0.30%) and it was thus considered that the viscoelastic behaviour should be approximately linear.

In the time range 10^{-8}–10 s, the creep compliances were derived from measurements[6] of the dynamic storage compliance $D'(\omega)$ at frequencies $f(=\omega/2\pi)$ between 0.01 Hz and 5 MHz. The dynamic techniques comprised[14] a tensile non-resonance method (0.01–60 Hz), audio-frequency flexural resonance (100 Hz to 4 kHz) and longitudinal resonance (5–12 kHz) methods, and an ultrasonic wave propagation technique (1–5 MHz). The very low strain amplitudes (1×10^{-4} to 6×10^{-2}%) in the dynamic experiments ensured that the viscoelastic behaviour was accurately linear. From the dynamic data, creep compliances at $t = 0.63/\omega$ were obtained using the approximation[5,6]:

$$D(0.63/\omega) = D'(\omega) \quad (6)$$

Data obtained by the different methods, after applying corrections for various effects, generally agreed to within 2%.

ANALYSIS OF SHORT-TERM CREEP DATA

Figure 1 shows short-term creep curves covering up to 13 decades of time for three PVC samples of different t_e. The data for $t_e = 10$ years were obtained on specimens from the original sheet. The elapsed time of 10 years is an estimate based on the storage time between receiving the sheet and performing the measurements, with the assumption that the material had been cooled from temperatures above T_g during processing just prior to receipt.

Good agreement is seen in *Figure 1* between data obtained by the different techniques. The time ranges corresponding to the secondary (β) retardation region and the onset of the glass–rubber (α) region are indicated. Only a small degree of overlap is observed between the α- and β-regions, a fairly well-defined plateau being evident at intermediate times. The level of the plateau, which corresponds to $D_{R\beta}$, decreases with increasing t_e.

The β-retardation region

In the β-region, the creep curves for PVC are quite symmetrical in shape (*Figure 1*). Following the method developed for other polymers[3,6], we have therefore modelled the data in this region using equations (1) (with $D_\alpha(t) = 0$) and (2). These equations predict that plots of $D(t)$ *versus* $\log t$ in the β-region are symmetrical about an inflection point at time τ_β.

In fitting the equations to the PVC data, τ_β values were first derived from experimental plots of dynamic loss compliance D'' *versus* $\log f$ using $\tau_\beta = 0.63\tau_c = 0.63/2\pi f_{max} = 0.1/f_{max}$. Here τ_c is the Cole–Cole retardation time and f_{max} is the frequency of maximum D'' for the β-process. From the D''–$\log f$ plots shown in *Figure 2* we find that f_{max}, and hence τ_β, is essentially independent of t_e and obtain $\tau_\beta = 10^{-5.1}$ s. The shape of the loss peak in *Figure 2*, and thus the value of n, also seems largely unaffected by ageing. However, the decrease in area of the peak with increasing t_e is consistent with a decrease in ΔD_β which is also evident in *Figure 1*.

Regarding the t_e dependence of ΔD_β, *Figure 3* shows plots of $\log[D(t) - D_{U\beta}]$ *versus* $\log t_e$ at different

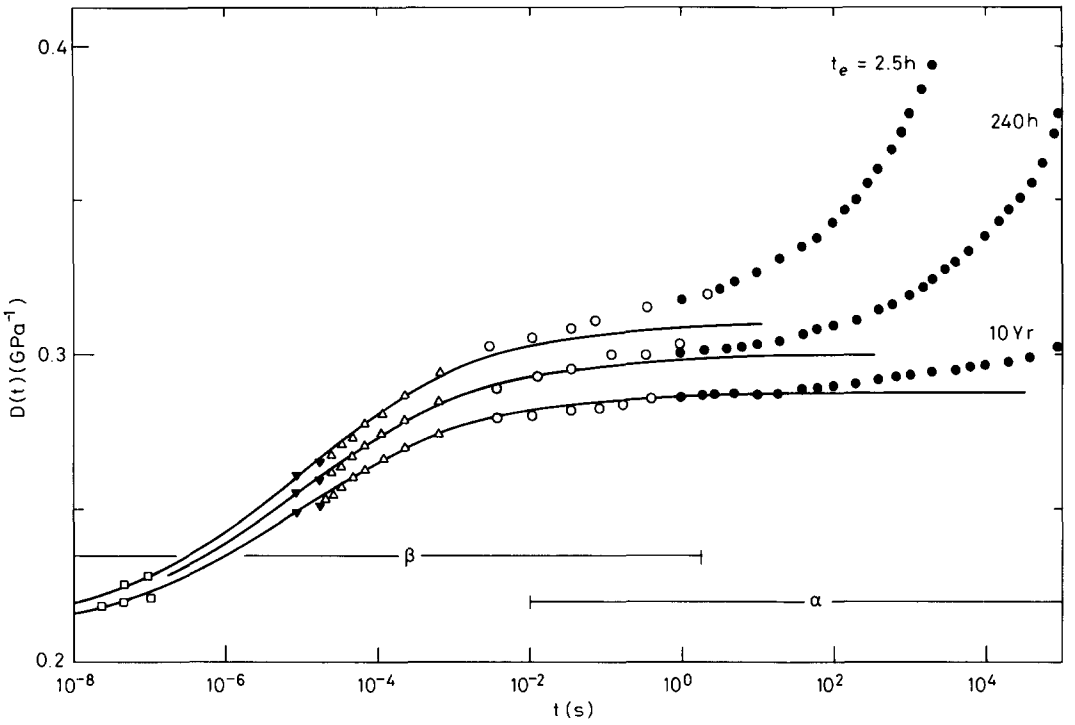

Figure 1 Creep curves at 23°C for PVC at different states of physical ageing characterized by the elapsed time t_e after quenching from 85°C. The techniques used to obtain the data were: □, ultrasonic wave propagation; ▼, audiofrequency longitudinal resonance; △, audiofrequency flexural resonance; ○, tensile non-resonance; ●, tensile creep. α and β indicate the time ranges over which the α- and β-retardation processes are active. The theoretical curves (——) were calculated using equations (1), (2) and (7), with $D_\alpha(t) = 0$, and represent the estimated β-contributions to the creep

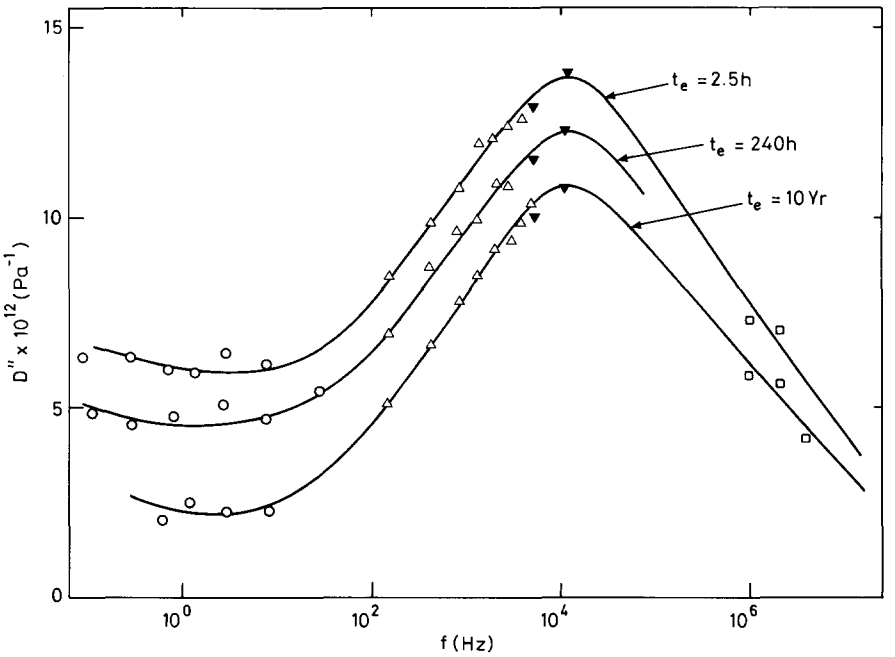

Figure 2 Tensile loss compliance D'' as a function of frequency f in the β-region for three elapsed times t_e. Symbols as in *Figure 1*

(essentially constant) creep times corresponding to various audiofrequency resonance modes of vibration. A value of $D_{U\beta} = 0.210\ \text{GPa}^{-1}$ was estimated from the very short time data in *Figure 1* and was assumed to be independent of t_e. It will be noted that the plots in *Figure 3* are linear and parallel and correspond to short times at which $D_\alpha(t)$ is probably negligible. In terms of equations (1) and (2), with τ_β, n and hence $\psi_\beta(t)$ independent of t_e, this result is consistent with the relationship:

$$\Delta D_\beta = Bt_e^{-k} \tag{7}$$

Here B and k are constants, the value $k = 0.024$ being obtained as the gradient of the lines in *Figure 3*. Using the values of τ_β, $D_{U\beta}$ and k given above, B and n values were then determined by optimizing the fits of equations (1) and (2) to creep data over the time range 10^{-8} to 10^{-3} s for which $D_\alpha(t)$ was considered negligible.

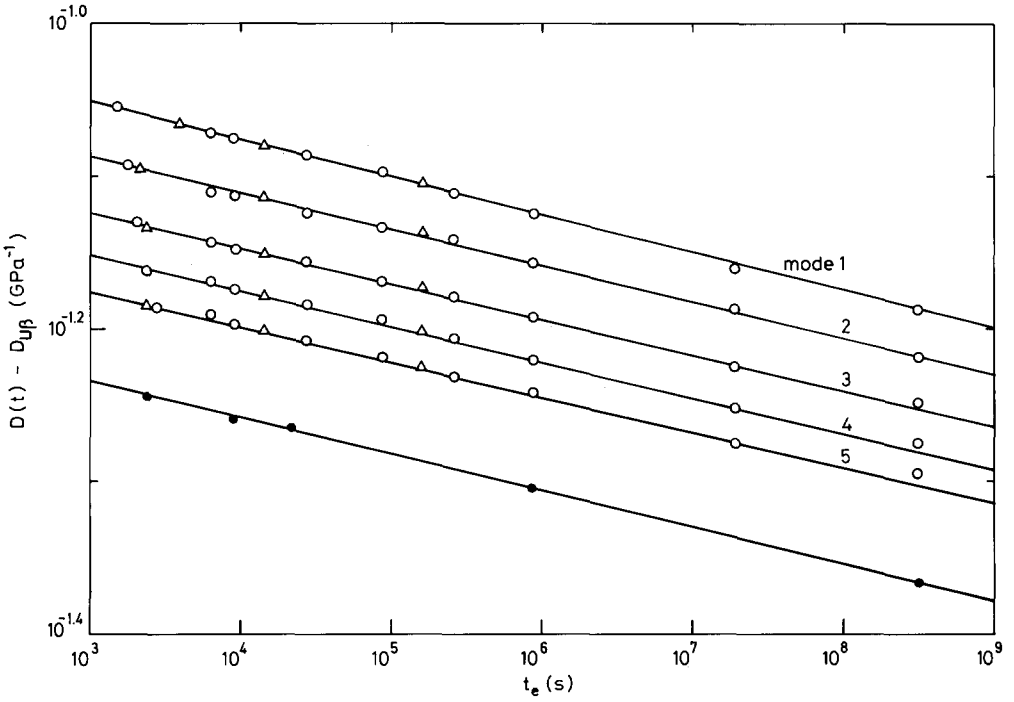

Figure 3 Plots of $\log[D(t) - D_{U\beta}]$ *versus* $\log t_e$ at six constant creep times t in the β-region: ○, data for a water-quenched sample from flexural resonance measurements on mode 1 ($t = 6.6 \times 10^{-4}$ s), mode 2 ($t = 2.3 \times 10^{-4}$ s), mode 3 ($t = 1.2 \times 10^{-4}$ s), mode 4 ($t = 7.2 \times 10^{-5}$ s) and mode 5 ($t = 4.8 \times 10^{-5}$ s); △, corresponding flexural resonance data for an air-quenched sample; ●, data for a water-quenched sample from longitudinal resonance measurements on mode 1 ($t = 1.8 \times 10^{-5}$ s)

Figure 1 illustrates the fits obtained to data at three elapsed times with $B = 0.125\ \text{GPa}^{-1}\ \text{s}^k$ and $n = 0.35$.

With regard to the structural significance of these results, *Figure 3* shows that data obtained for the air-quenched PVC specimen agree well with results for the water-quenched material. This indicates that the results were not influenced by the existence of any internal stresses in the specimens[7]. Furthermore, the value of 0.024 for k suggests that ΔD_β, and hence the number of relaxing groups responsible for the β-process, decreases by 5.5% per decade of elapsed time. Since τ_β and n are essentially independent of t_e, the mobilities of those groups which remain active are unchanged.

One interpretation of these results is that the active groups reside in certain loosely-packed regions which are slowly eliminated by main-chain rearrangements involved in the ageing process[9]. The results may alternatively be considered in terms of Struik's theory of secondary relaxations[15]. This is based on the two-potential-well model and accounts for the coupling of relaxing groups to the glassy environment. According to this theory (equation (5.62) of ref. 15) the number of active 'type 2' groups, and hence ΔD_β, is approximately proportional to $\exp -(\Delta E/4RT_g)$. Here ΔE is the coupling energy ($\Delta E \gg RT_g$) and it is assumed that the conformational energy ΔU_0 for an isolated group is zero. During physical ageing, a decrease in the number of type 2 groups could thus occur through slow rearrangements of the environment producing a decrease in T_g (the structural or fictive temperature) and a possible increase in ΔE. Assuming that T_g decreases by 2 K (or 0.6%) per decade of elapsed time[16] and that $\Delta E/4RT_g \approx 3$ (ref. 15), then ΔD_β would decrease by 5.5% per decade of elapsed time for an increase in ΔE of about 1.2%. Since these changes in T_g and ΔE would have a negligible effect[15] on τ_β, our results may be consistent with Struik's theory. Note, however, that Struik failed to detect any change in ΔD_β with age state and suggested that each relaxing group is completely coupled to its environment (implying that ΔE is unaffected by ageing).

The α-retardation region

The compliance contribution $D_\alpha(t)$ in short-term tests was obtained using equation (1) by subtracting extrapolated values of $D_{U\beta} + D_\beta(t)$, derived with the aid of equations (2) and (7), from the measured $D(t)$. The resulting α-creep curves covered only the short-time tail of the α-region where $(t/\tau_\alpha)^m \ll 1$ and equation (3) becomes:

$$\log D_\alpha(t) = \log \Delta D_\alpha + m \log t - m \log \tau_\alpha \qquad (8)$$

This equation predicts that plots of $\log D_\alpha(t)$ *versus* $\log t$ should be linear and of slope m. Such plots for PVC at different elapsed times (*Figure 4*) were linear and parallel within experimental error and thus yielded an m value (0.324) which is independent of t_e. Some departure from linearity at short creep times is ascribed to the magnification of experimental errors in determining very small $D_\alpha(t)$ values. The constancy of m implies that the width of the α-retardation spectrum is unaffected by ageing.

Since the plots in *Figure 4* are parallel, it also follows that they can be superposed by either: (a) vertical shifts, corresponding to a decrease in ΔD_α with increasing t_e at constant τ_α; or (b) horizontal shifts, corresponding to an increase in τ_α with increasing t_e at constant ΔD_α; or (c) a combination of vertical and horizontal shifts. Therefore it is not possible to establish from the short-term data whether ageing involves changes in ΔD_α, τ_α or both. However the long-term creep behaviour, which is considered in a subsequent section, can help to distinguish between the different ageing effects. As a basis for the long-term creep predictions, the data in *Figure 4* have been modelled in terms of cases (a) and (b) above.

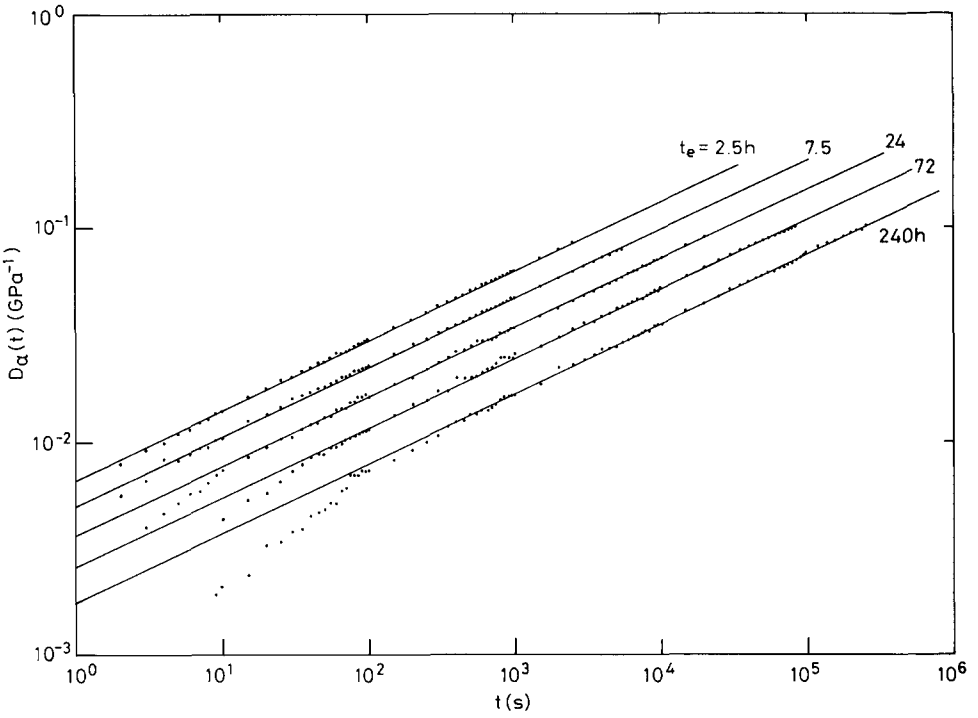

Figure 4 Log $[D_\alpha(t)]$ *versus* log t from short-term tests at different elapsed times t_e. The straight lines each have a gradient $m = 0.324$

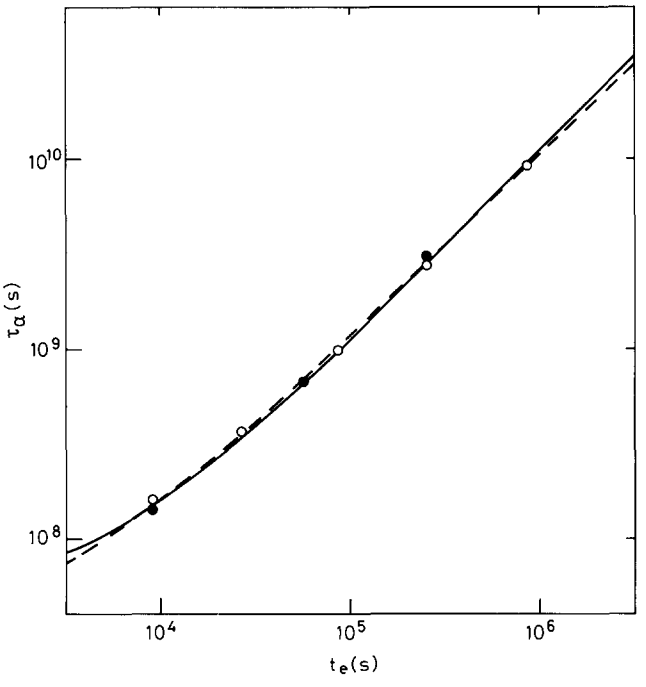

Figure 5 Log τ_α *versus* log t_e: ○, data from short-term creep tests; ●, results from the short-term regions of long-term tests; ——, calculated using equation (11) with $\mu = 1$, $A_{1W} = 5 \times 10^7$ s and $A_{2W} = 1.08 \times 10^4$; – – – –, calculated using equation (11) with $\mu = 0.95$, $A_{1W} = 3 \times 10^7$ s and $A_{2W} = 2.07 \times 10^4$ s$^{1-\mu}$

With these analyses it was recognized that equation (3) should apply only to the short-time part of the glass–rubber region arising from local segmental motions[17,18]. It could not describe the behaviour over those parts of the region attributed to longer range Rouse–Bueche chain modes. Since contributions to $D_\alpha(t)$ from the local process are not well understood the chosen values for ΔD_α and the corresponding τ_α must be arbitrary. However, values of ΔD_α between about $10D_{R\beta}$ and $100D_{R\beta}$ were considered appropriate, since these are substantially less than the total compliance change ($\approx 1000D_{R\beta}$) typically obtained for the glass–rubber process. It should also be noted that the time range over which equation (3) can accurately model the data is insensitive to the ΔD_α value employed.

Case (a): ΔD_α *variable*, τ_α *constant*. In this case a value $\Delta D_\alpha = 3$ GPa$^{-1} \approx 10D_{R\beta}$ was selected for $t_e = 2.5$ h. A value of $\tau_\alpha = 1.60 \times 10^8$ s was then derived from the intercept (log $\Delta D_\alpha - m \log \tau_\alpha$) in *Figure 4*, obtained by extrapolating the plot for $t_e = 2.5$ h to the ordinate at log $t = 0$. Assuming that this value of τ_α is independent of t_e, the ΔD_α values for other t_e values were determined from the other intercepts in *Figure 4*. It was found that log ΔD_α decreases approximately linearly with log t_e suggesting a relationship of the form:

$$\Delta D_\alpha = Qt_e^{-r} \tag{9}$$

where $r = 0.293$ and $Q = 45.0$ GPa^{-1} s^r.

Case (b): τ_α *variable*, ΔD_α *constant*. Using an arbitrary constant value of 3 GPa^{-1} for ΔD_α, the value of τ_α at each t_e value was determined from the intercepts at log $t = 0$ in *Figure 4*. A plot of log τ_α *versus* log t_e (*Figure 5*) is slightly curved with a gradient which increases somewhat with increasing t_e. Over limited ranges of t_e, the plot is approximately linear and can be fitted by the equation:

$$\tau_\alpha = A_W t_e^{\mu_a} \tag{10}$$

with the constants A_W and μ_a dependent on the t_e range considered. Values for the apparent ageing rate μ_a increase, for example, from 0.83 for the t_e range 2.5–24 h to 0.90 for the t_e range 2.5–240 h. These results are consistent with the observations of Striuk[10] which further

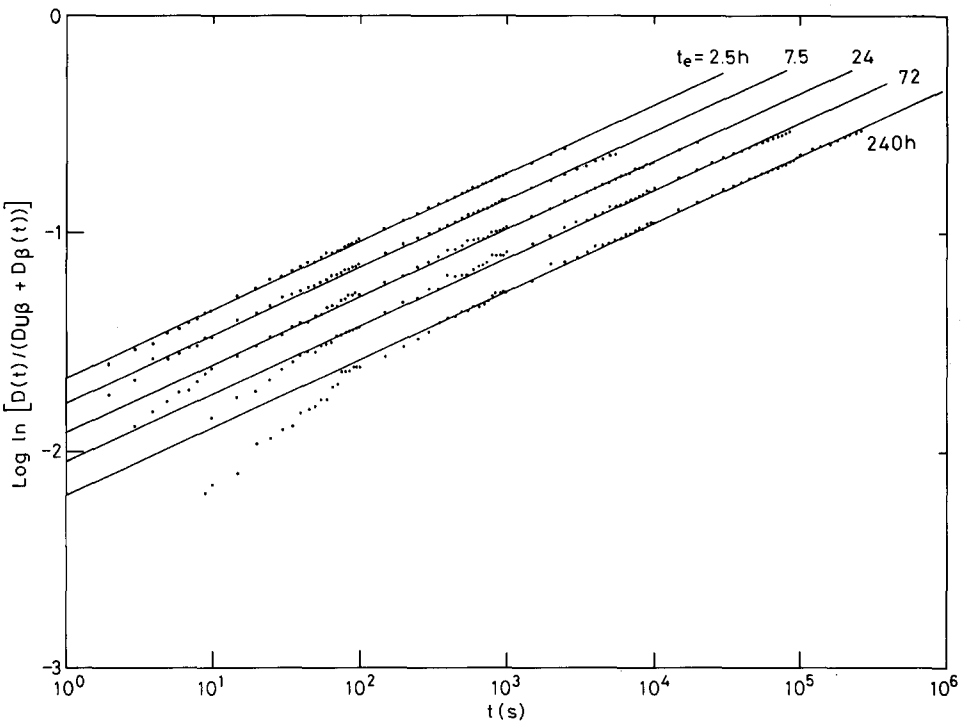

Figure 6 Plots of log $\ln\{D(t)/[D_{U\beta} + D_\beta(t)]\}$ *versus* log t from short-term tests in the α-region at different elapsed times t_e. The straight lines each have a gradient $\gamma = 0.31$

suggest that the log τ_α–log t_e plot becomes accurately linear at long t_e with a gradient close to unity. On this basis the equation:

$$\tau_\alpha = A_{1W} + A_{2W}t_e^\mu \qquad (11)$$

where A_{1W}, A_{2W} and μ are constants, has been used to model the variation of τ_α over a wide range of t_e. Note that A_{1W} corresponds to the retardation time immediately following the quench ($t_e = 0$) and that μ is the slope of the log τ_α–log t_e plot in the linear region at long t_e. Plots of τ_α *versus* t_e^μ were approximately linear using $\mu = 1$ and Struik's value[10] of $\mu = 0.95$, so that values of A_{2W} could be obtained as the slopes and A_{1W} as the intercepts at $t_e = 0$. *Figure 5* gives the values of these parameters and illustrates the fits obtained to the log τ_α–log t_e plots.

Application of the Struik–Kohlrausch function. Assuming that ΔD_α is unaffected by ageing, and need not be considered in the analysis, the creep behaviour in the α-region can also be modelled according to equation (4). Since this can be expressed in the form:

$$\log\ln\{D(t)/[D_{U\beta} + D_\beta(t)]\} = \gamma\log t - \gamma\log t_o \qquad (12)$$

it predicts that plots of $\log\ln\{D(t)/[D_{U\beta} + D_\beta(t)]\}$ *versus* log t should be linear and of slope γ. *Figure 6* shows that the plots for PVC are linear and parallel, except for the region at short times where the function $\log\ln\{D(t)/[D_{U\beta} + D_\beta(t)]\}$ is subject to large experimental error. From these plots we obtain $\gamma = 0.31$ and again deduce that the distribution parameter is essentially independent of t_e. The value of t_o at each t_e was obtained from the intercept produced by extrapolating the plot to the ordinate at $\log t = 0$ or to the abscissa at $\log\ln\{D(t)/[D_{U\beta} + D_\beta(t)]\} = 0$.

The log t_o–log t_e plot (*Figure 7*) exhibits a slight curvature similar to that in *Figure 5* but over limited t_e ranges it can be modelled approximately by the equation:

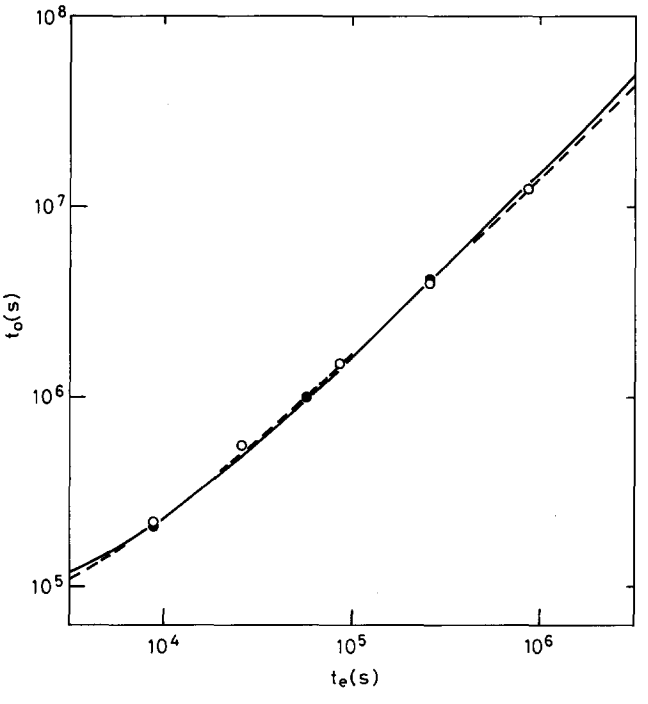

Figure 7 Dependence of the relaxation time, t_o, upon the elapsed time t_e: ○, results from short-term creep tests; ●, data from the short-term regions of long-term tests; ——, calculated using equation (14) with $\mu = 1$, $A_{1S} = 7 \times 10^4$ s, $A_{2S} = 15.8$; – – – –, calculated using equation (14) with $\mu = 0.95$, $A_{1S} = 5 \times 10^4$ s, $A_{2S} = 29.1$ s$^{1-\mu}$

$$t_o = A_S t_e^{\mu_a} \qquad (13)$$

where the constants A_S and μ_a depend on the t_e range considered and μ_a values are, within experimental error, equal to those obtained using equation (10). Over wide ranges of t_e the variation of t_o with t_e can be described by:

$$t_o = A_{1S} + A_{2S}t_e^\mu \qquad (14)$$

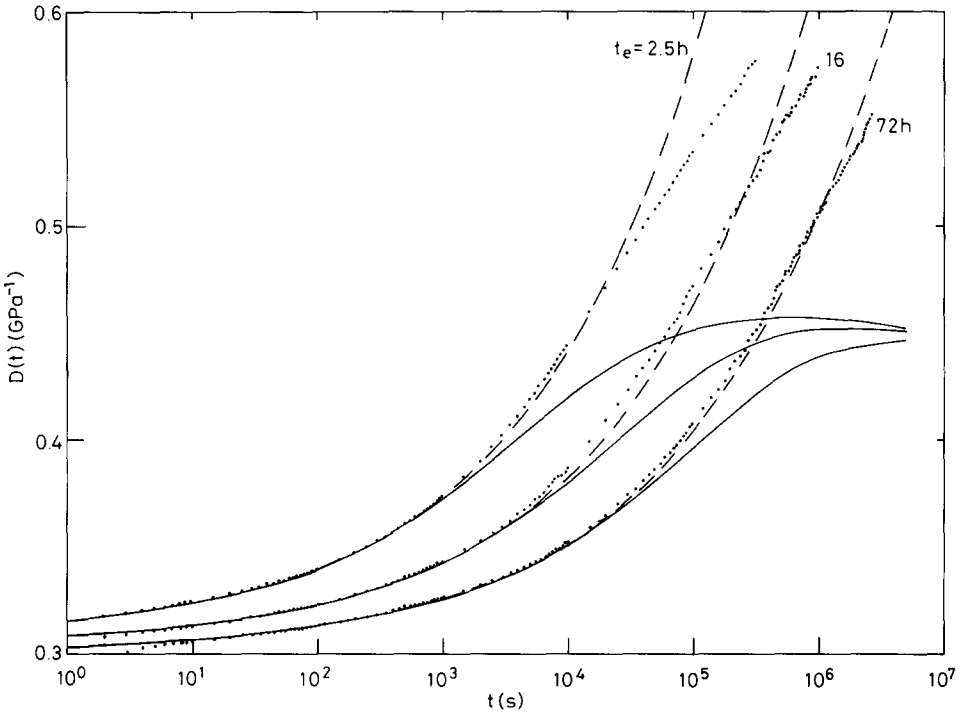

Figure 8 Long-term creep curves for three elapsed times t_e: ·, experimental data; ——, predicted curves based on equations (1), (16) and (17); – – – –, extrapolated short-term data according to equations (1), (2), (3), (7) and (9). Values used for parameters as follows: $D_{U\beta} = 0.21\ \text{GPa}^{-1}$, $\tau_\beta = 7.94 \times 10^{-6}$ s, $n = 0.35$, $B = 0.125\ \text{GPa}^{-1}\ \text{s}^k$, $k = 0.024$, $Q = 45.0\ \text{GPa}^{-1}\ \text{s}^r$, $r = 0.293$, $\tau_\alpha = 1.60 \times 10^8$ s, $m = 0.324$

where A_{1S}, A_{2S} and μ are constants, A_{1S} corresponding to the value of t_0 at $t_e = 0$. The constant μ is the slope of the log t_0–log t_e plot at long t_e and has the same value as μ in equation (11). Plots of t_0 *versus* t_e^μ were used to obtain A_{1S} (from the intercept) and A_{2S} (from the slope). As illustrated in *Figure 7*, a slightly closer fit of equation (14) to the data was obtained using Struik's value of $\mu = 0.95$ than with $\mu = 1$.

ANALYSIS OF LONG-TERM CREEP DATA

During long-term tests ($t > 0.2t_e$) significant further ageing accompanies the creep deformation. Modifications are then required to the expressions for $D_\beta(t)$ and $D_\alpha(t)$ to allow for progressive variations in certain of the retardation parameters.

For the β-process, the analysis of short-term data suggests that, whilst τ_β and n are essentially constant, ΔD_β will decrease with increasing time during the long-term creep. Equation (2) must then be replaced by[6]:

$$D_\beta(t) = \Delta D_\beta(0)\psi_\beta(t) + \int_0^t \psi_\beta(t-u)\frac{\mathrm{d}}{\mathrm{d}u}\Delta D_\beta(u)\,\mathrm{d}u \tag{15}$$

where $\Delta D_\beta(0)$ is the value of ΔD_β at $t = 0$ and the integral accounts for changes in ΔD_β during the creep. From equation (7) we write $\Delta D_\beta(0) = Bt_e^{-k}$ and $\Delta D_\beta(u) = B(t_e + u)^{-k}$. For times $t \gg \tau_\beta$, $\psi_\beta(t-u) \approx \psi_\beta(t)$ over most of the time interval $u = 0 - t$. Equation (15) then simplifies to:

$$D_\beta(t) = B(t_e + t)^{-k}\psi_\beta(t) \tag{16}$$

From the analysis of short-term data for the α-process, it is evident that ageing during long-term creep could involve either: (a) a decrease in ΔD_α at constant τ_α and m; or (b) an increase in τ_α at constant ΔD_α and m; or (c) variations in both ΔD_α and τ_α. The extent to which the different ageing mechanisms may be involved has been explored by comparing experimental long-term creep curves with predicted curves for cases (a) and (b).

Case (a): ΔD_α variable, τ_α and m constant

In this case equation (3) is replaced by[6]:

$$D_\alpha(t) = \Delta D_\alpha(0)\psi_\alpha(t) + \int_0^t \psi_\alpha(t-u)\frac{\mathrm{d}}{\mathrm{d}u}\Delta D_\alpha(u)\,\mathrm{d}u \tag{17}$$

where $\Delta D_\alpha(0)$ is the value of ΔD_α at $t = 0$ and the integral accounts for the possible decrease in ΔD_α with increasing creep time. From equation (9) we have $\Delta D_\alpha(0) = Qt_e^{-r}$ and $\Delta D_\alpha(u) = Q(t_e + u)^{-r}$. After substituting these relations into equation (17), together with expressions for $\psi_\alpha(t)$ and $\psi_\alpha(t-u)$ according to equation (3), values of $D_\alpha(t)$ were obtained with the aid of numerical integrations.

In *Figure 8*, experimental long-term creep data for three t_e values are compared with the predicted curves using equations (1), (16) and (17). Also shown are curves corresponding to extrapolations of the short-term data assuming no further ageing. All parameters were obtained from the analyses of short-term data and are given in the figure caption. Note that the predicted long-term compliances are substantially lower than the experimental values. The rapid convergence at long times of the predicted curves for different t_e is also inconsistent with the experimental data. These discrepancies could arise partly from an inability of the function $\psi_\alpha(t)$ to provide an accurate basis for extrapolating data to the long-term region. However, they are considered largely to reflect an overestimate of the ageing effects associated with the assumption of a t_e-dependent ΔD_α.

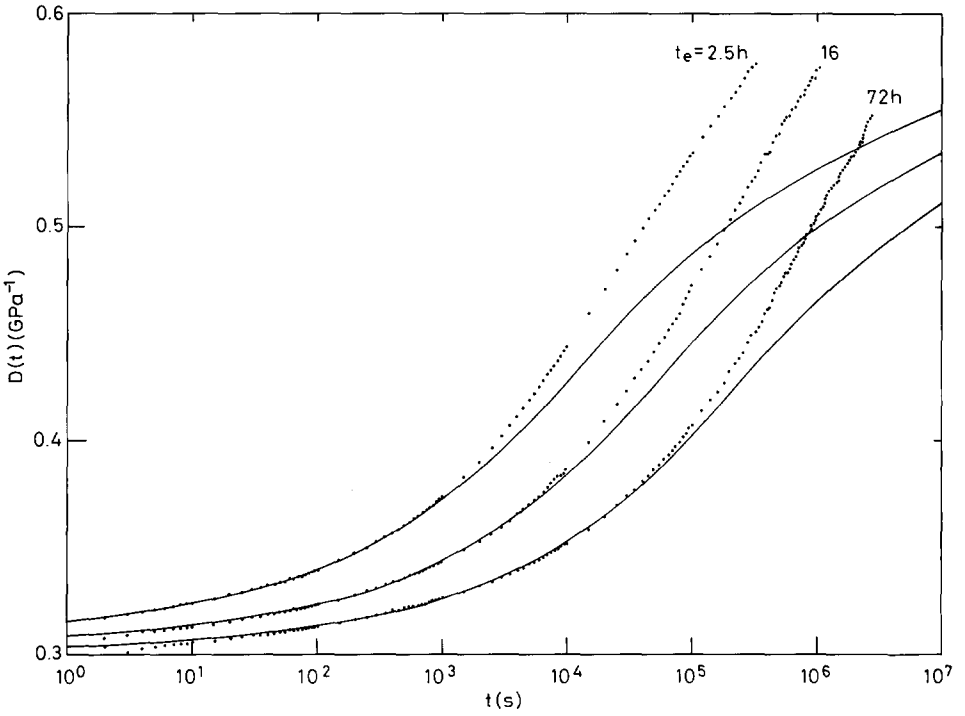

Figure 9 Long-term creep curves for three elapsed times t_e: ·, experimental data; ——, predicted curves using equations (1), (16), (18) and (20) with $\Delta D_\alpha = 3\ \mathrm{GPa}^{-1}$, $A_{1W} = 5 \times 10^7$ s, $A_{2W} = 1.08 \times 10^4$, $m = 0.324$. Values used for $D_{U\beta}$, τ_β, n, B and k as in *Figure 8*

Case (b): τ_α variable, ΔD_α and m *constant*

To predict the long-term creep behaviour in this case, we replace equation (3) by[6]:

$$D_\alpha(t) = \Delta D_\alpha[1 - \exp - I_W^m] \tag{18}$$

where the integral

$$I_W = \int_0^t \frac{du}{\tau_\alpha(u)}$$

allows for the increase in τ_α during the creep deformation.

In the long-term regions of the creep curves for $t_e = 16$ and 72 h, the *total* elapsed times $(t_e + t)$ become considerably longer than 72 h. It is evident that the μ value at these elapsed times is close to unity (*Figure 5*) and that an equation such as (11) is required to model the variations of τ_α over the wide ranges of total elapsed time in the long-term tests. Using equation (11) the integral becomes:

$$I_W = \int_0^t \frac{du}{A_{1W} + A_{2W}(t_e + u)^\mu} \tag{19}$$

For $\mu = 1$, this equation has the solution:

$$I_W = \frac{1}{A_{2W}} \ln\left(1 + \frac{A_{2W}t}{A_{1W} + A_{2W}t_e}\right) \tag{20}$$

Figure 9 shows long-term creep curves predicted from the short-term parameters with $\mu = 1$ using equations (1), (16), (18) and (20). The predicted curves now show little tendency to converge in the long-term region, in agreement with the experimental curves, but the predicted compliances are again lower than the measured compliances. Since improved fits could be obtained by allowing m to increase with creep time, these discrepancies may largely reflect inadequacies in the Williams–Watts function $\psi_\alpha(t)$ as a basis for extrapolating short-term data to longer times in the glass–rubber region of amorphous polymers. Note, however, that the long-term data are significantly closer to the case (b) than to the case (a) predictions. This suggests that the ageing is associated predominantly with an increase in α-retardation time, and that any changes in ΔD_α are probably small or negligible.

Application of the Struik–Kohlrausch function

In applying the Struik–Kohlrausch function to the analysis of long-term creep, we replace equation (4) by:

$$D(t) = [D_{U\beta} + D_\beta(t)] \exp I_S^\gamma \tag{21}$$

where

$$I_S = \int_0^t \frac{du}{t_0(u)}$$

Using equation (14) to model the variation of t_0 with total elapsed time in long-term tests we then obtain:

$$I_S = \int_0^t \frac{du}{A_{1S} + A_{2S}(t_e + u)^\mu} \tag{22}$$

For $\mu = 1$, equation (22) has the solution:

$$I_S = \frac{1}{A_{2S}} \ln\left(1 + \frac{A_{2S}t}{A_{1S} + A_{2S}t_e}\right) \tag{23}$$

Figure 10 includes long-term creep curves predicted from short-term data with $\mu = 1$ using equations (16), (21) and (23). Although the predicted compliances are somewhat lower than the observed compliances, the agreement between theory and experiment is within 6% and is substantially closer than that in *Figure 9*. Also shown in *Figure 10* are long-term curves calculated using parameters from short-term data with $\mu = 0.95$. These calculations involved equations (16) and (21) together with the numerical integration of (22). For $t_e = 16$ and 72 h, the predicted long-term compliances are 1–2%

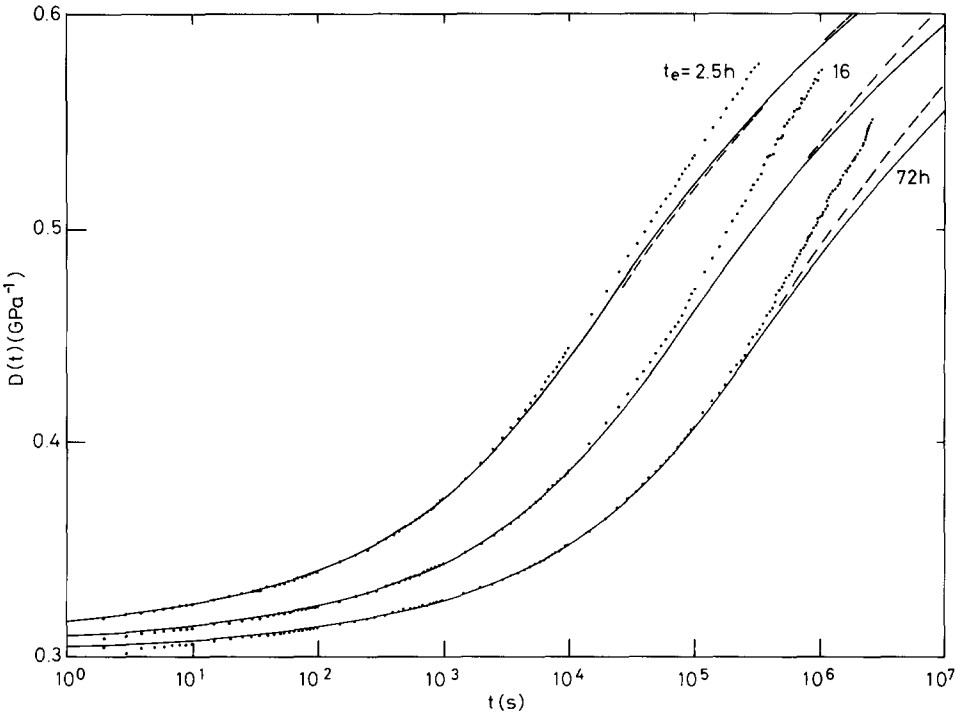

Figure 10 Long-term creep curves for three elapsed times t_e: ·, experimental data; ——, predicted curves using equations (16), (21) and (23) with $A_{1S} = 7 \times 10^4$ s, $A_{2S} = 15.8$, $\gamma = 0.31$; – – – –, predicted curves using equations (16), (21) and (22) with $\mu = 0.95$, $A_{1S} = 5 \times 10^4$ s, $A_{2S} = 29.1\ s^{1-\mu}$, $\gamma = 0.31$. For each predicted curve, values used for $D_{U\beta}$, τ_β, n, B and k as in *Figure 8*

higher than those calculated with $\mu = 1$ and are thus slightly closer to the observed compliances.

The discrepancies in *Figure 10* between the observed and predicted long-term creep curves could partly involve inaccuracies in the form of the Struik–Kohlrausch function for extrapolating short-term curves to longer times (neglecting further ageing). This may be regarded in terms of a possible slight dependence of γ and t_o on creep time t. In this context, accurate fits to the long-term parts of the creep curves have been achieved using equations (21) and (23) with parameters ($\gamma = 0.33$, $A_{2S} = 11.5$) which differ somewhat from the 'short-term' parameters.

An alternative explanation for the discrepancies in *Figure 10* is that equations (22) and (23) do not allow for non-linear behaviour arising from stress-induced deageing. This could occur to some extent despite the low stress level of 5.1 MPa employed in the (static) creep tests. Our recent investigation of creep in PVC at high stresses[13] suggests that, for $\mu = 1$, equation (22) should be replaced by:

$$I_S = \int_0^t \frac{du}{A_{1S} + A_{2S}t_e} = \frac{t}{A_{1S} + A_{2S}t_e} \qquad t \leqslant t_m \quad (24a)$$

and

$$I_S = \int_0^{t_m} \frac{du}{A_{1S} + A_{2S}t_e} + \int_{t_m}^t \frac{du}{A_{1S} + A_{2S}t_e + A_{3S}(u - t_m)}$$

$$= \frac{t_m}{A_{1S} + A_{2S}t_e} + \frac{1}{A_{3S}} \ln\left[1 + \frac{A_{3S}(t - t_m)}{A_{1S} + A_{2S}t_e}\right]$$

$$t > t_m \quad (24b)$$

Here t_m marks the end of the time interval during which t_o is essentially constant, or passes through a broad minimum, following an initial rapid deageing (decrease in t_o) by the stress. The parameter A_{3S} equals the derivative dt_o/dt during the subsequent reactivation of ageing and relates to the magnitude of the initial deageing. Note that $A_{3S} \leqslant A_{2S}$, that A_{3S} and t_m each depend on stress and t_e, and that in the limit of zero stress t_m vanishes and A_{3S} becomes equal to A_{2S}.

Figure 11 shows long-term creep curves calculated using equations (16), (21), (24a) and (24b) with $\gamma = 0.31$ and $A_{2S} = 15.8$ obtained from short-term data. Values of t_m were estimated as the times at which deviations from linearity were first apparent in plots of $[\ln\{D(t)/[D_{U\beta} + D_\beta(t)]\}]^{1/\gamma}$ *versus* t. This procedure follows from the fact that the slopes of these plots give the instantaneous values of $1/t_o$ during the creep test[13]. Values of A_{3S} were then chosen to optimize the fits of equations (16), (21) and (24b) to the long-term data. *Figure 11* illustrates that the long-term creep behaviour can be accurately modelled with realistic values of A_{3S}. Further investigations at very low stress and/or elevated temperatures should help to confirm the accuracy of the Struik–Kohlrausch function in describing the creep of amorphous polymers in the short-time tail of the glass–rubber region.

CONCLUSIONS

Creep curves obtained for PVC at 23°C and at times t between 10^{-8} and 10^6 s have been modelled with some success in terms of compliance contributions from overlapping secondary (β) and glass–rubber (α) processes. Each contribution depends on the physical age of the polymer as specified by the elapsed time t_e at 23°C between quenching from 85°C and the instant of loading.

The β-contribution has been described satisfactorily by a symmetrical function (equation (2)) derived from the Cole–Cole equation. Physical ageing gives rise to a decrease in strength ΔD_β of the β-retardation, consistent

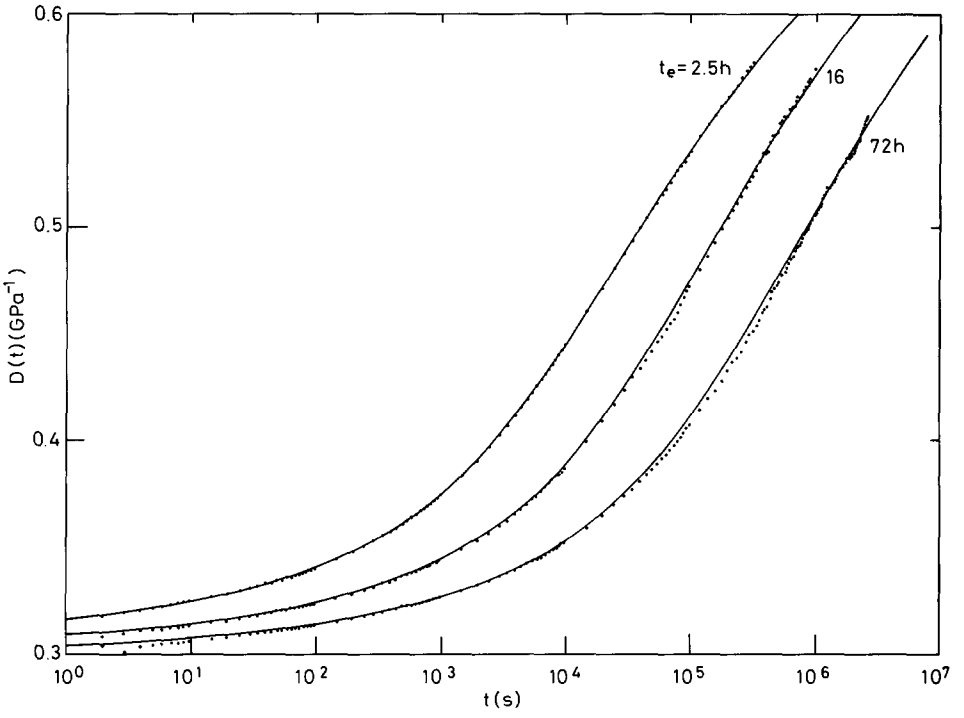

Figure 11 Long-term creep curves for three elapsed times t_e: ·, experimental data; ——, calculated curves using equations (16), (21), (24a) and (24b) with $A_{1S} = 7 \times 10^4$ s, $A_{2S} = 15.8$, $\gamma = 0.31$ and values for t_m and A_{3S} as follows: $t_e = 2.5$ h, $t_m = 1 \times 10^3$ s, $A_{3S} = 12.5$; $t_e = 16$ h, $t_m = 1 \times 10^4$ s, $A_{3S} = 10.5$; $t_e = 72$ h, $t_m = 3 \times 10^4$ s, $A_{3S} = 10.0$. For each calculated curve, values used for $D_{U\beta}$, τ_β, n, B and k as in *Figure 8*

with a reduction in the number of active groups of 5.5% per decade of elapsed time. However, the mean β-retardation time and width of the distribution are unchanged.

In the α-region, the short-term creep curves ($t \leqslant 0.2t_e$) can be described in terms of functions of the Williams–Watts (equation (3)) or the Struik–Kohlrausch (equation (4)) forms. Analyses of short-term data suggest that physical ageing has a negligible effect on the width of the α-retardation time distribution but could produce either a decrease in the magnitude of ΔD_α or an increase in the mean retardation time, or both. However, analyses of long-term data ($t > 0.2t_e$) suggest that ageing principally involves an increase in mean retardation time at constant ΔD_α. The long-term creep behaviour has been accurately modelled on the basis of the Struik–Kohlrausch function after allowing for possible deageing effects of the applied stress (5.1 MPa).

REFERENCES

1 Read, B. E., Tomlins, P. E. and Dean, G. D. *Polymer* 1990, **31**, 1204
2 Read, B. E., Dean, G. D. and Tomlins, P. E. *Plast. Rubber Process. Appl.* 1990, **14**, 153
3 Dean, G. D., Read, B. E. and Small, G. D. *Plast. Rubber Process. Appl.* 1988, **9**, 173
4 Dean, G. D., Read, B. E. and Tomlins, P. E. *Plast. Rubber Process. Appl.* 1990, **13**, 37
5 Read, B. E. *J. Non-Cryst. Solids* 1991, **131–133**, 408
6 Read, B. E., Dean, G. D. and Tomlins, P. E. *Polymer* 1988, **29**, 2159
7 Struik, L. C. E. *Polymer* 1987, **28**, 57
8 Diaz-Calleja, R., Ribes-Greus, A. and Gomez-Ribelles, J. L. *Polymer* 1989, **30**, 1433
9 Johari, G. P. in 'Molecular Dynamics and Relaxation Phenomena in Glasses' (Eds Th. Dorfmüller and G. Williams), Lecture Notes in Physics 277, Springer-Verlag, Berlin, 1987, p. 90
10 Struik, L. C. E. 'Physical Aging in Amorphous Polymers and Other Materials', Elsevier, Amsterdam, 1978
11 Plazek, D. J., Ngai, K. L. and Rendell, R. W. *Polym. Eng. Sci.* 1984, **24**, 1111
12 Leaderman, H. 'Elastic and Creep Properties of Filamentous Materials and other High Polymers', The Textile Foundation, Washington, DC, 1944, pp. 13–14
13 Dean, G. D., Read, B. E., Lesniarek-Hamid, J. L. and Tomlins, P. E. NPL Report DMM(A)17, National Physical Laboratory, Teddington, 1990
14 Read, B. E. and Dean, G. D. 'The Determination of Dynamic Properties of Polymers and Composites', Adam Hilger, Bristol, 1978
15 Struik, L. C. E. in 'Molecular Dynamics and Relaxation Phenomena in Glasses' (Eds Th. Dorfmüller and G. Williams), Lecture Notes in Physics 277, Springer-Verlag, Berlin, 1987, p. 27
16 Kovacs, A. J. *J. Polym. Sci.* 1958, **30**, 131
17 Ngai, K. L., Plazek, D. J. and Deo, S. S. *Macromolecules* 1987, **20**, 3047
18 Fytas, G. and Ngai, K. L. *Macromolecules* 1988, **21**, 804